

ESI – Myszka et al.

Electronic Supplemental Information for

Phase-specific bioactivity and altered Ostwald ripening pathways of calcium carbonate polymorphs in simulated body

Barbara Myszka^a, Martina Schüßler^b, Katrin Hurle^c, Benedikt Demmert^b, Rainer Detsch^a, Aldo R. Boccaccini^{a,d}, and Stephan E. Wolf^{b,d,*}

a. Institute of Biomaterials, Friedrich-Alexander-University of Erlangen-Nuremberg, Cauerstrasse 6, 91058 Erlangen, Germany.

b. Institute for Glass and Ceramics, Friedrich-Alexander-University Erlangen-Nuremberg, Martensstraße 5, 91058 Erlangen, Germany.

c. GeoZentrum Nordbayern – Mineralogy, Friedrich-Alexander-University Erlangen-Nuremberg, Schlossgarten 5a, 91054 Erlangen, Germany.

d. Interdisciplinary Center for Functional Particle Systems (FPS), Friedrich-Alexander-University Erlangen-Nuremberg, 91058 Erlangen, Germany.

* To whom correspondence should be addressed: stephan.e.wolf@fau.de

Section A — Calcite

Phase purity of commercial calcite

The phase purity of the commercially supplied calcite is documented by XRD (Fig. A1-A), with the highest intensity representing (104) at $2\theta = 29.3^\circ$. All other peaks also belong to calcite, i.e. (113), (116), (018), (202), (110), (012), (1010) and (215). Thermal analysis of the powder (Fig. A1-B) showed only weight loss above 700°C which relates to thermal decomposition of calcium carbonate; and it corresponds also to the endothermic peak in the DTA curve. Prior to this event, no weight loss or other endo-/exothermic events can be identified which assures the absence of organic substances or a potentially amorphous phase. The overall weight loss is 43–44% which is in agreement with the theoretical loss of 44 wt% [1]. The ATR/FT-IR spectrum of the powder (Fig. A1-C) shows the characteristic absorption bands of calcite: the in-plane band (ν_4) at 711 cm^{-1} , the out plane band (ν_2) at 876 cm^{-1} , and an anti-symmetry stretch (ν_3) at 1402 cm^{-1} [2]. It is worth mentioning that sharp bands at 876 cm^{-1} confirm phase-pure calcite because the out-of-plane band (ν_2) of aragonite is at 854 cm^{-1} and for vaterite at 867 cm^{-1} [3]. Raman spectroscopy studies also showed the characteristic bands of calcite and no bands of a second polymorph (Fig. A1-D). The single band at 1085 cm^{-1} is related to internal modes that originates from the ν_1 symmetric stretching mode of the carbonate ion. The ν_4 in-plane-bending mode of carbonate can be found at 711 cm^{-1} . Bands below 300 cm^{-1} correspond to translational and rotational lattice modes [4].

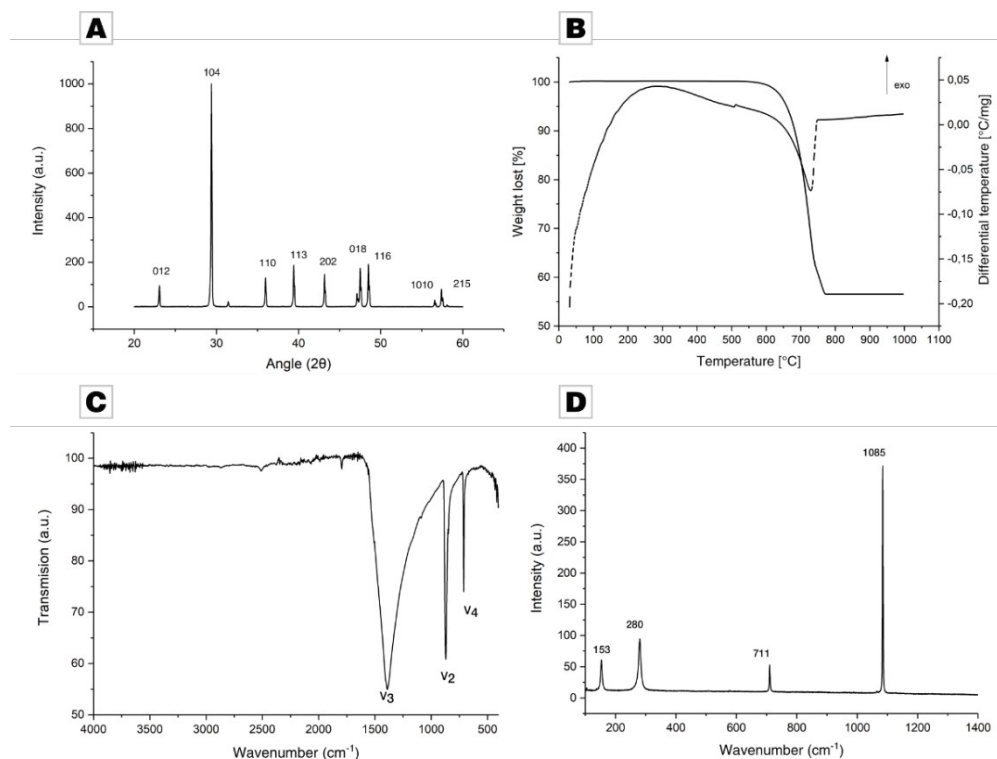


Figure A1. Characterization of commercial calcite. (A) X-ray diffraction, (B) TGA/DTA analysis, (C) ATR/FT-IR spectroscopy, and (D) Raman spectroscopy.

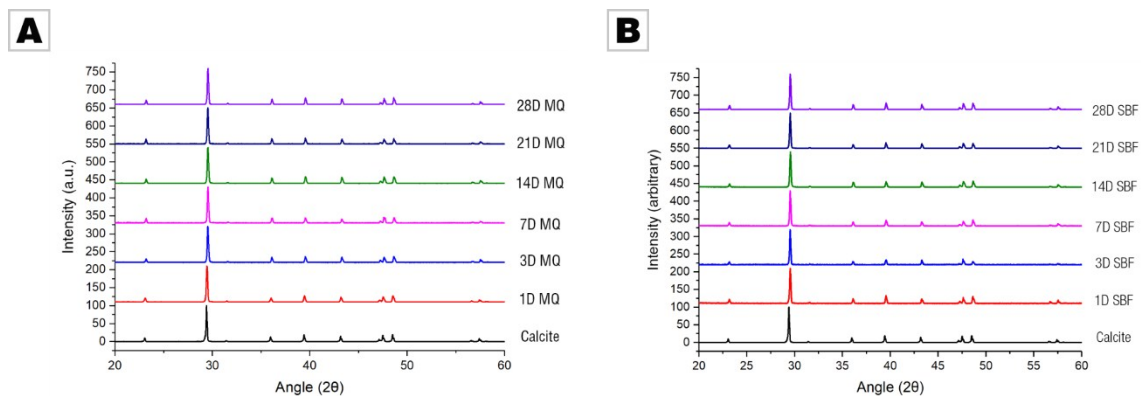


Figure A2. Evolution of X-ray diffractograms of calcite during incubation (A) in water and (B) in SBF for a time period of up to 28 d. Throughout, only reflections from calcite are present.

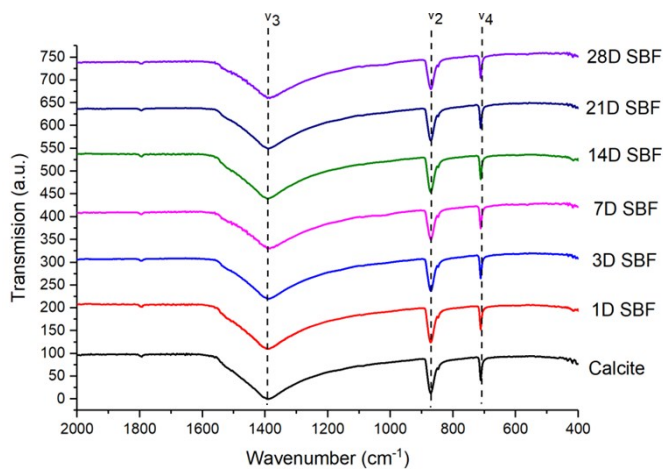


Figure A3. Evolution of ATR/FT-IR spectra of calcite during incubation in SBF for a time period of up to 28 d. No characteristic phosphate bands are present even after 4 weeks.

Section B — Aragonite

Phase purity of synthesized aragonite

The phase purity of aragonite was assured by XRD (Fig. B1-A), where the analysis shows that all the diffraction peaks are in accordance with the standard data PDF No. 00-041-1475 [5]. Thermal analysis of the precipitated powder (Fig. B1-B) showed a first weight loss of ~ 0.5 – 1.0 wt% below 100 °C which is due to the elimination of physically adsorbed water. The second weight loss of 1.0 – 2.0 wt% at 240 – 400 °C is due to the elimination of occluded water. The thermal decomposition at the temperature range 550 – 750 °C; the overall weight loss and the absence of further endo- or exothermic events indicates that only one phase pure of organic impurities is present. The ATR/FTIR spectrum of the sample (Fig. B1-C) features the anti-symmetry stretching vibration (ν_3) at 1460 cm^{-1} , a symmetric carbonate stretching vibration (ν_1) at 1084 cm^{-1} and a carbonate out-of-plane bending (ν_2) vibration at 854 cm^{-1} which are all characteristic of the aragonite structure [6]. In aragonite, the symmetric stretching vibration (ν_1) is active both in Raman and IR whereas in the case of calcite it is only Raman-active. Often, this band at ~ 1080 cm^{-1} is used to discriminate aragonite from mixtures of aragonite and calcite [7]. The pair of bands at ca. 713 and 700 cm^{-1} are assigned to the in-plane bending modes (ν_4) which are also characteristic for aragonite [6,8]. No characteristic vibrational bands belonging to calcite or vaterite were detected, which further demonstrate that the powder obtained is pure aragonite. The Raman spectrum presents (Fig. B1-D) the strongest line in the ν_1 symmetric stretch of CO_3^{2-} ion at ~ 1084 cm^{-1} . A pair of bands presented at 700 and 704 cm^{-1} are characteristic of aragonite [9]. Bands below 300 cm^{-1} corresponded to translational and rotational lattice modes [10].

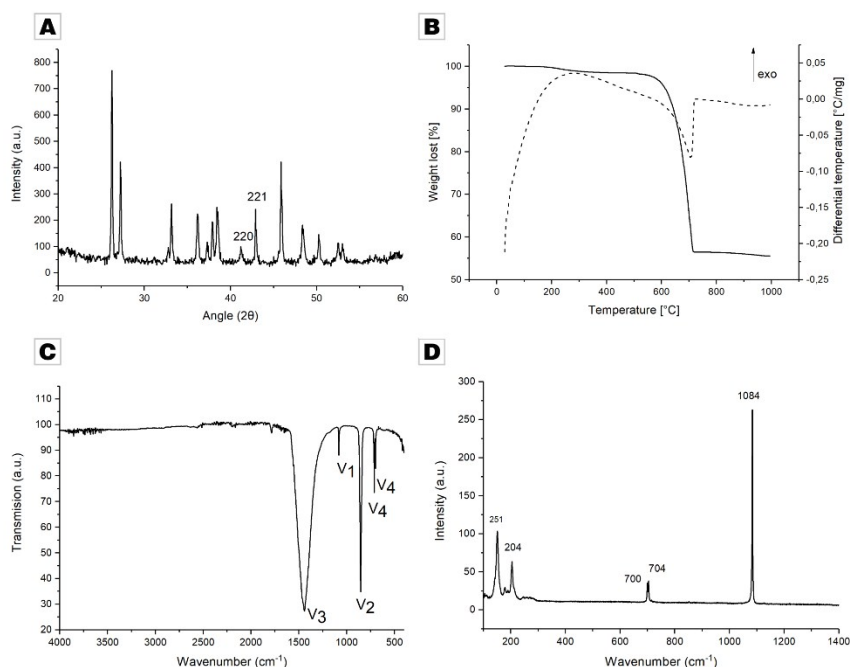


Figure B1. Characterization of synthesized aragonite. (A) X-ray diffraction, (B) TGA/DTA analysis, (C) ATR/FT-IR spectroscopy, and (D) Raman spectroscopy.

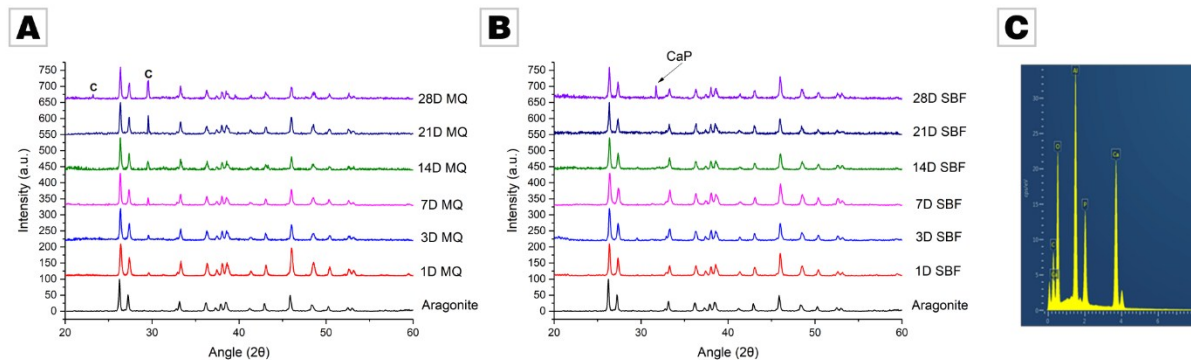


Figure B2. Evolution of X-ray diffractograms of aragonite before/during incubation (A) in water and (B) in SBF for a time period of up to 28 d. Only after 28 d, a small peak of calcium phosphate is present. No calcite appears. (C) EDS of spherulitic precipitates, as marked in Fig. 2-B.

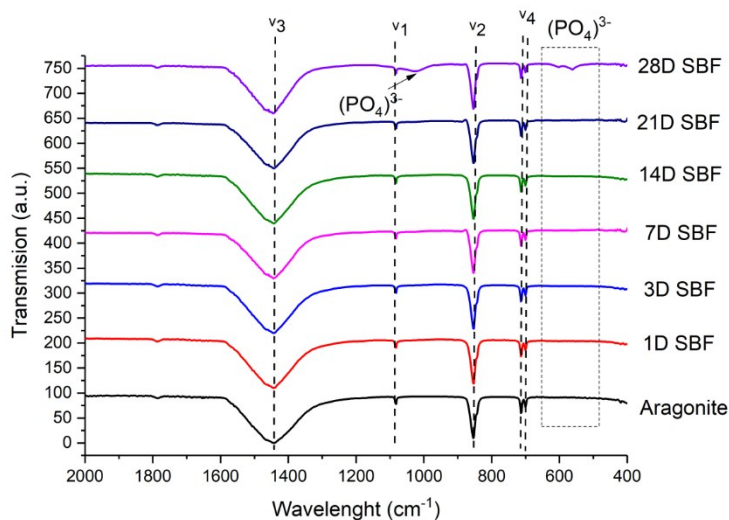


Figure B3. Evolution of ATR/FT-IR spectra of aragonite before/during incubation in SBF for a time period of up to 28 d. Only after 28 d, a small peak of calcium phosphate is present. No calcite appears; however, after 28 days of incubation absorption bands typical for phosphate groups at 1029, 601 and 563 cm^{-1} appear additionally to the bands of aragonite.

Table B4. Rietveld refinement for aragonite powder after 1–28 days of immersion into MilliQ water.

	wt% calcite	wt% aragonite
1 day	3	97
3 days	4	96
7 days	4	96
14 days	8	92
21 days	11	89
28 days	18	82

Section C — Vaterite

Phase purity of synthesized vaterite

Vaterite was synthesized by a double decomposition technique and its phase purity was documented by XRD (Fig. C1-A) which is in agreement with the standard data PDF NO. 00-033-0268 [5]. The precipitated powder was characterized by TG-DTA analysis (Fig. C1-B) where the first slow weight loss shows a total of 0.5 wt% which we attribute to the evaporation of the physically adsorbed water [11]. The second weight loss of 1.0–1.5 wt% at 150–450 °C is due to the elimination of occluded water in vaterite, similar to the observations made in case of aragonite. The last weight lost in the temperature of 500–800 °C (~42.0 wt%) is due to decomposition of CaCO_3 to CaO and CO_2 and is accompanied by an endothermic peak at 715 °C in the DTA curve. The TGA/DTA analysis gave no evidence for a second, e.g. amorphous, phase and assured the absence of organic impurities. ATR/FTIR analysis (Fig. C1-C) only showed absorption bands characteristic of vaterite: 1090 cm^{-1} (ν_1 symmetric carbonate stretching vibration), 867 cm^{-1} (ν_2 a carbonate out-of-plane bending), 1409 cm^{-1} (ν_3 anti-symmetry stretch) and 736 cm^{-1} (ν_4 in-plane bending). No bands belonging to aragonite at 713 and 700 cm^{-1} , or calcite at 711 and 876 cm^{-1} were detected, further corroborating that ellipsoidal polycrystals are vaterite [8,12]. Raman spectroscopy studies also showed only bands characteristic of vaterite (Fig. C1-D). [10] Raman bands at 1073 and 1089 cm^{-1} correspond to the internal mode that derives from the ν_1 symmetric stretching mode of the carbonate ion. At 738–750 cm^{-1} the ν_4 in-plane bending mode of carbonate can be found. Samples exhibit bands below 300 cm^{-1} , which correspond to translational and rotational lattice modes.

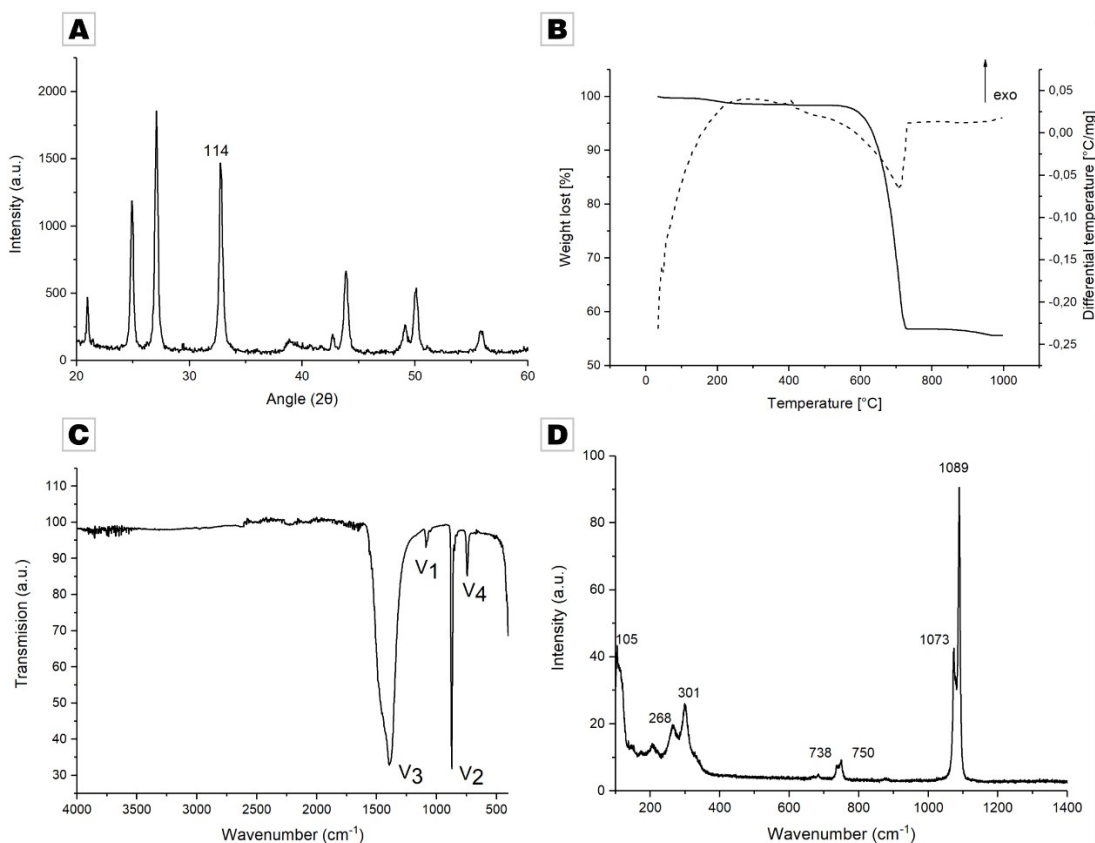


Figure C1. Characterization of synthesized vaterite. (A) X-ray diffraction, (B) TGA/DTA analysis, (C) ATR/FT-IR spectroscopy, and (D) Raman spectroscopy.

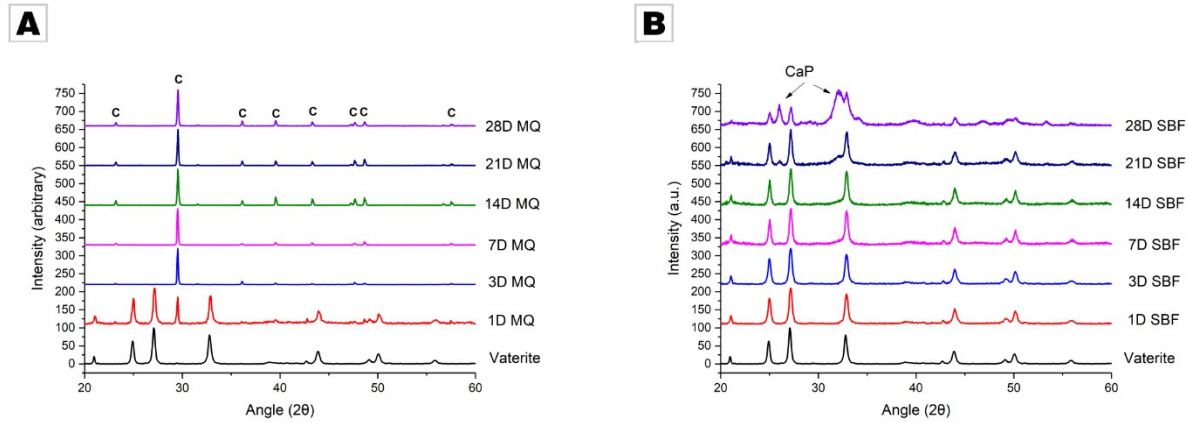


Figure C2. Evolution of X-ray diffractograms of vaterite before/during incubation (A) in water and (B) in SBF for a time period of up to 28 d. Only after 28 d, a small peak of calcium phosphate is present. Already after one day of incubation in water, calcite reflections appear additional to those of vaterite; after 3 d all vaterite reflection have vanished. In contrast, no calcite formation is detectable in SBF but calcium phosphate reflections are detectable after 28 d of incubation.

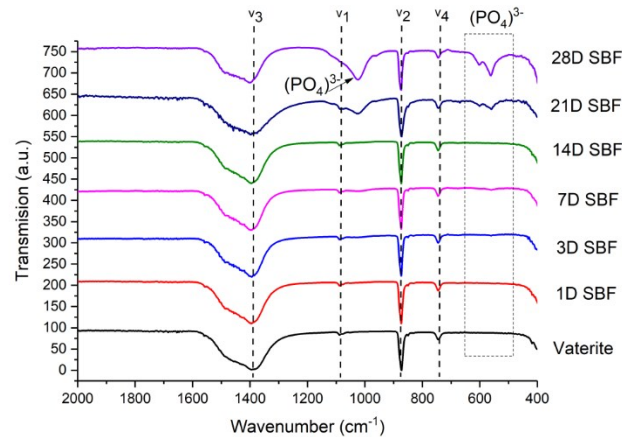


Figure C3. Evolution of ATR/FT-IR spectra of vaterite before/during incubation in SBF for a time period of up to 28 d. After 28 days of incubation, absorption bands typical for calcium phosphate at 1029, 601 and 563 cm⁻¹ appear additionally to the bands of vaterite.

Section D – Amorphous Calcium Carbonate

Phase purity of synthesized amorphous calcium carbonate (ACC)

The dried ACC precipitate is X-ray amorphous (Fig. D1-A); only diffuse scattering is observed which is common for ACC phase and was already previously reported.^{10,11} TGA/DTA showed an initial weight loss up to 300–460 °C which is attributed to loss of water (~15.0 wt. %, Fig. D1-B). The initial dehydration step, below 120 °C, represents the loss of physisorbed water and the further loss between 120–460 °C is related to bound water. A remarkable exothermic DTA signal occurred at around 390 ± 3 °C. Since this event was accompanied by only a minor increase in weight loss which is probably due to increased release of structural water, it denotes a recrystallization event of the ACC to a crystalline phase, probably calcite. Above 500 °C, dramatic weight loss occurs due to the decomposition of calcite into CaO and CO₂.¹⁰ At this point, the DTA curve exhibits an endothermic peak centered at 680 °C corresponding to the decarbonation of calcite.¹⁴ The FT-IR spectrum (Fig. D1-C) presents the significant bands of ACC at 865 cm⁻¹ (ν_2 , the carbonate out-of-plane bending), and 1080 cm⁻¹ (ν_1 , the symmetric stretch in the non-centrosymmetric structure) and the splitting of the 1425 cm⁻¹ (ν_3 , the asymmetric stretch) also validate the formation of the ACC phase.^{11,12} The absence of vibrations bands at 713 cm⁻¹ or 745 cm⁻¹, which are characteristic of crystalline calcium carbonate phases, indicates that the mineralized product is pure ACC. The broad absorption bands between 3000 and 3600 cm⁻¹ (O–H stretching) and a sharper band at 1632 cm⁻¹ (O–H bending) can be assigned to structural water in ACC.¹² The Raman spectrum (Fig. D1-D) does not exhibit distinct bands in the spectrum region of 70–360 cm⁻¹ belonging to the lattice modes, whereas the ν_1 band is located at 1080 cm⁻¹, which provides further support for the assumption that the particles are indeed ACC.¹³

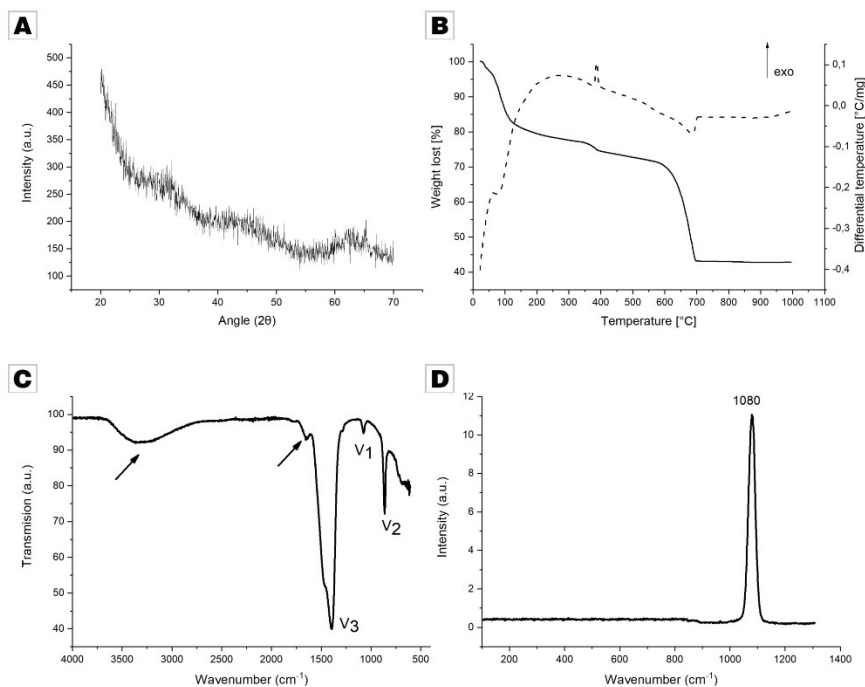


Figure D1. Characterization of synthesized amorphous calcium carbonate (ACC). (A) X-ray diffraction, (B) TGA/DTA analysis, (C) ATR/FT-IR spectroscopy, and (D) Raman spectroscopy.

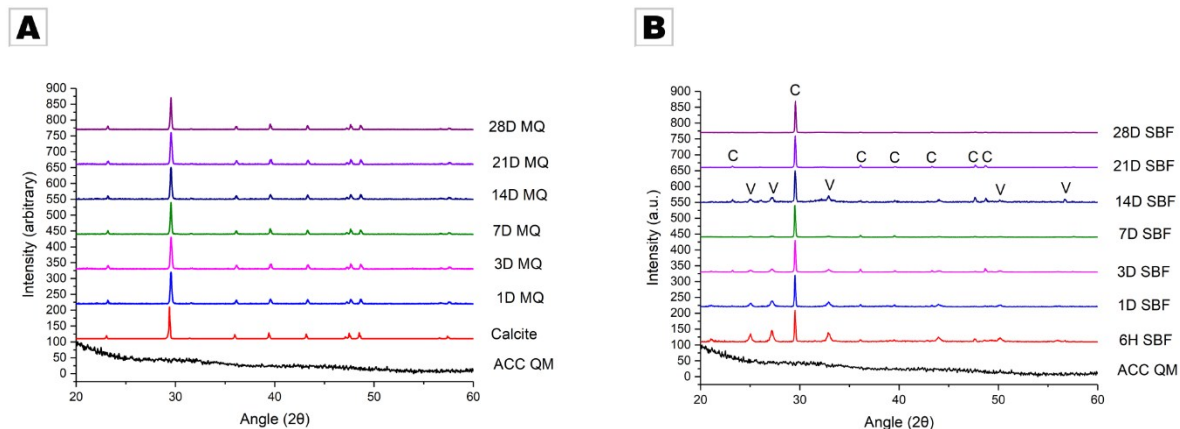


Figure D2. Evolution of X-ray diffractograms of ACC before/during incubation (A) in water and (B) in SBF for a time period of up to 28 d. Already after 1 d, only calcite is detectable.

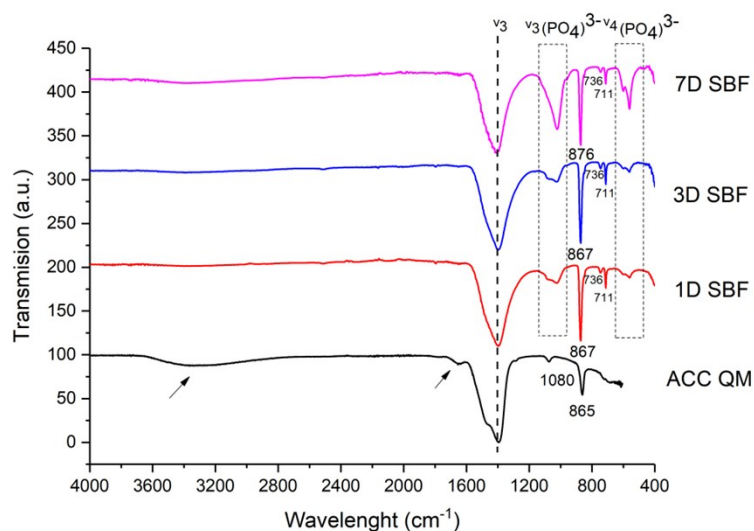


Figure D3. Evolution of ATR/FT-IR spectra of ACC before/during incubation in SBF for a time period of up to 7 d. Upon immersion, characteristic bands of calcite appear; already after 1 d absorption bands typical for phosphate appear. Arrows mark the broad absorption peak between 3000 and 3600 cm^{-1} (O–H stretching) and a sharper band at 1632 cm^{-1} (O–H bending) which are assigned to water structurally bound in ACC.

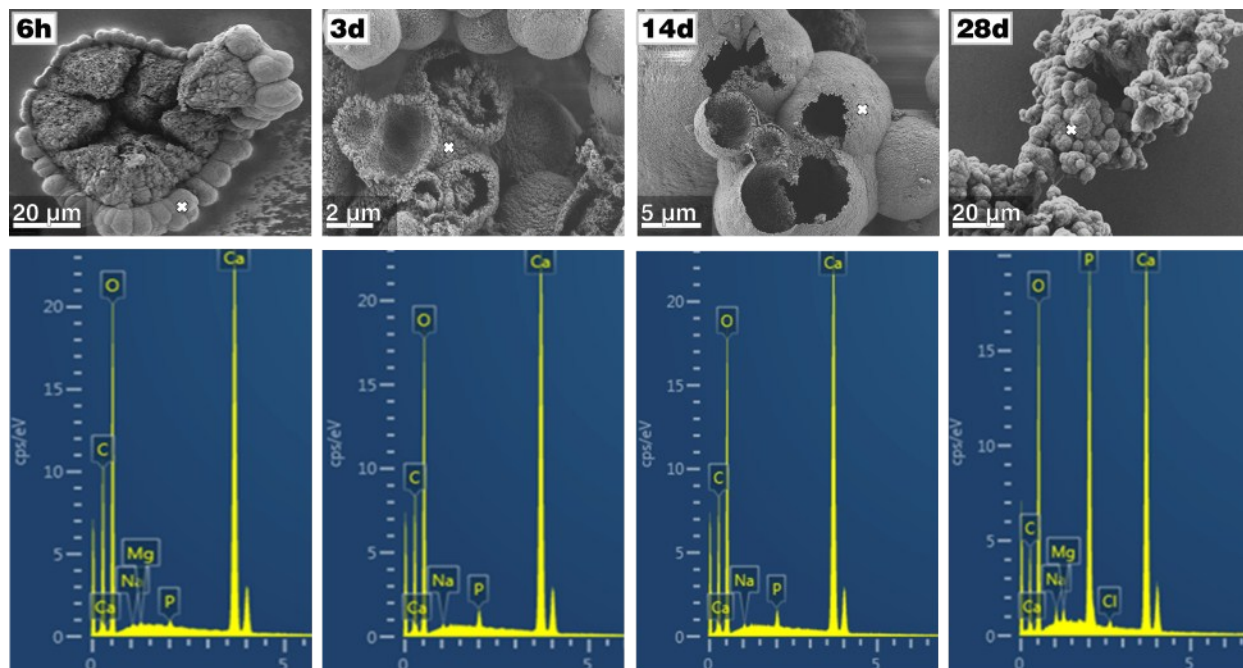


Figure D.4. EDS analysis of hollow-sphere morphologies formed during incubation of ACC in SBF solution. Already after 6 h, signals of phosphorus are detectable.

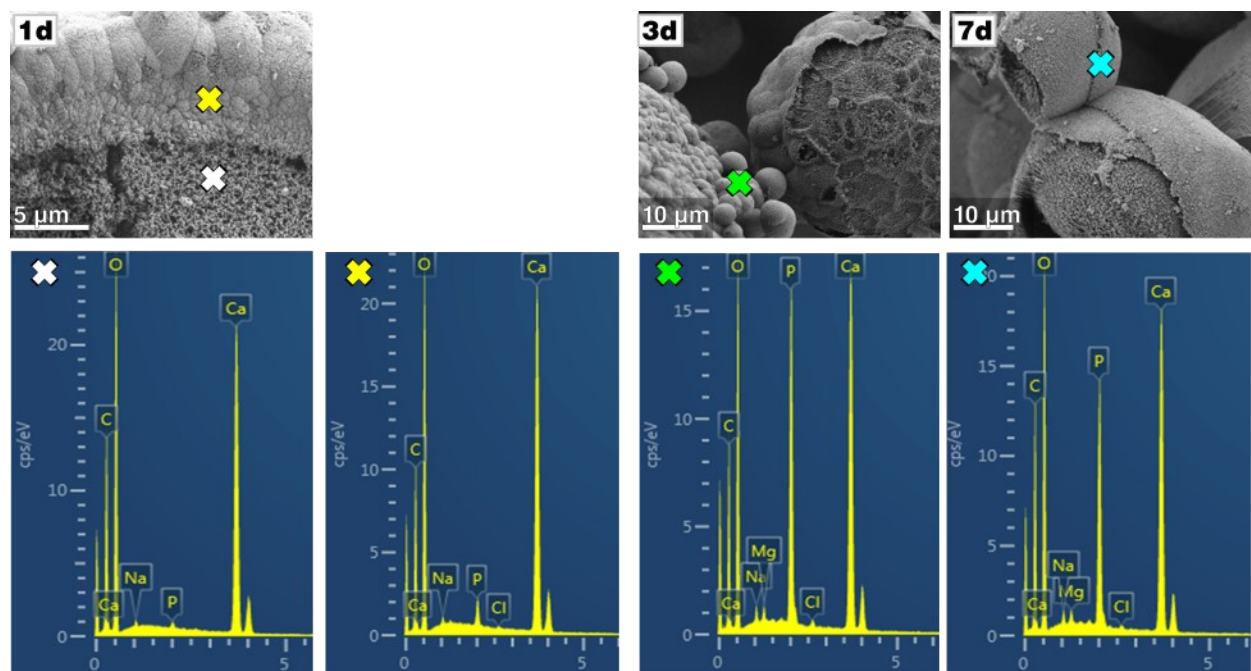


Figure D5. SEM micrographs and EDS analysis of hollow-sphere morphologies formed during incubation of ACC in 10x mSBF solution. Already after 6 h, signals of phosphorus are detectable.

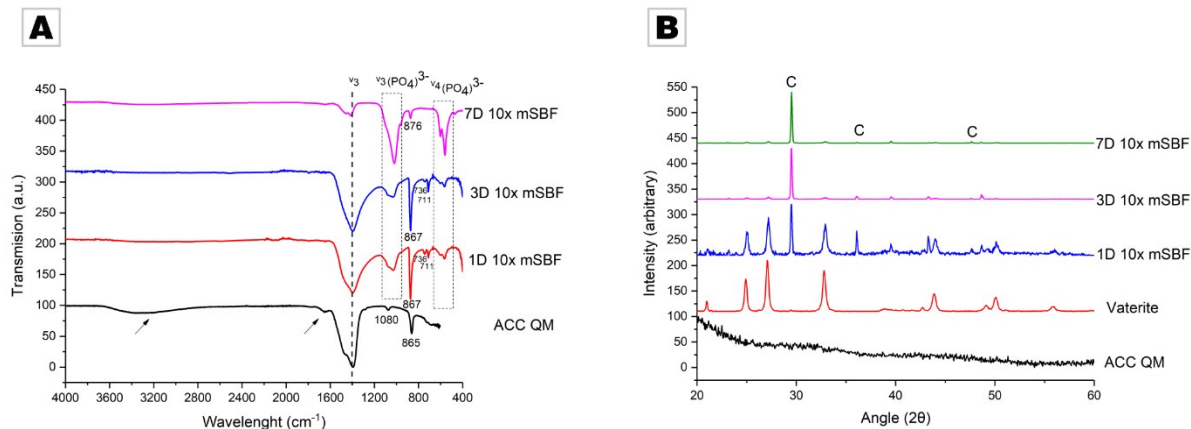


Figure D6. (A) ATR/FTIR spectra and (B) X-ray diffractograms of ACC before/after incubation in 10xSBF for a time period of up to 7 d. After 1 d, signals of vaterite and calcite are present; after 3 d, only calcite is detectable. After one day of immersion, the IR spectra show absorption bands of phosphate appear, i.e., anti-symmetry stretch vibration (ν_3) at 1029 cm⁻¹ and in-plane bending (ν_4) at 601 and 563 cm⁻¹. Arrows indicate the broad absorption peak between 3000 and 3600 cm⁻¹ (O–H stretching) and a sharper band at 1632 cm⁻¹ (O–H bending) which are assigned to water structurally bound in ACC.

Table D7. Ion content of Ca²⁺, Mg²⁺ and Na⁺ in the different Mg-ACC powders, as determined by ICP-MS.

Sample	wt% Mg	wt% Ca	wt% Na
ACC_10Mg	0.87	31	0.8
ACC_20Mg	2.6	29	1
ACC_40Mg	5.7	32	0.7

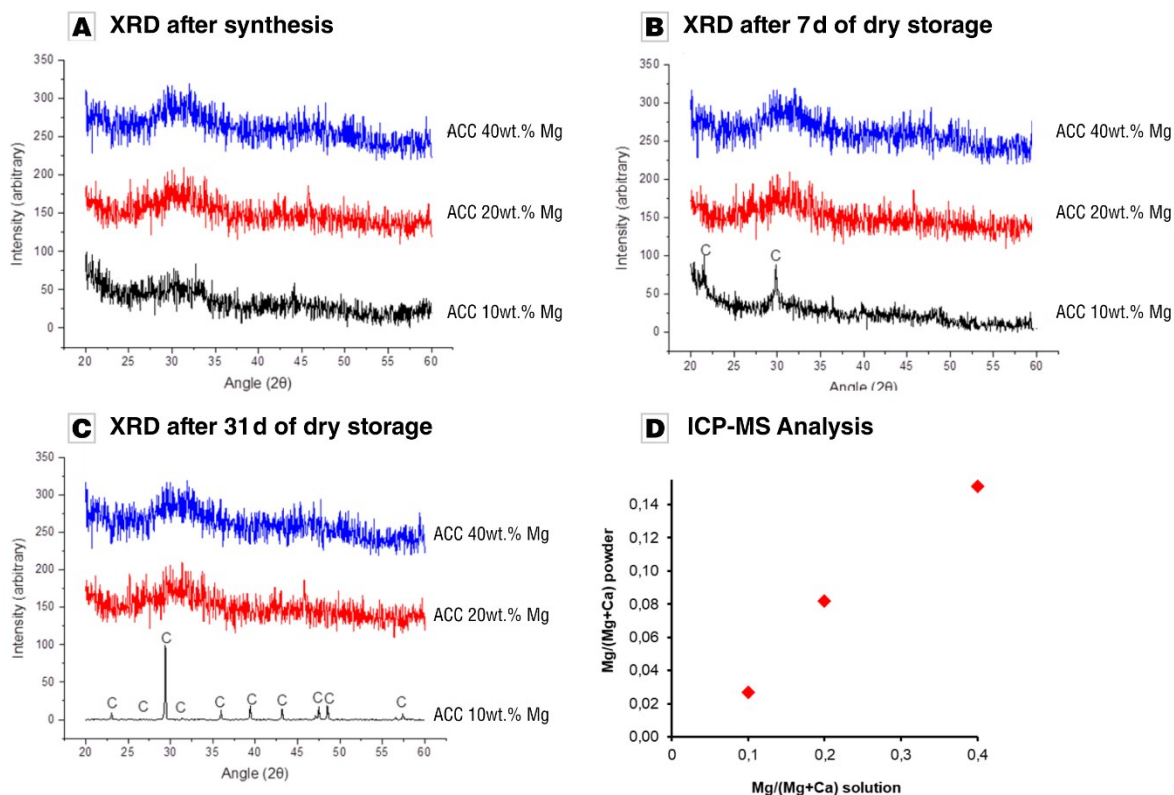


Figure D8. Analysis of Mg-doped ACC. (A-C) X-ray diffractograms of Mg-doped ACC (synthesized with 10, 20, 40 wt% Mg), stored under dry conditions for a time period of up to 31 d. After 7 days of storage the sample with 10 wt% magnesium addition slowly starts to recrystallize to calcite, samples with 20 and 40 wt% magnesium addition after 31 days of storage are still fully amorphous. (D) Weight ratio Mg/(Mg + Ca) in the precipitated ACC powders as determined by ICP-OES, plotted against the ratio Mg/(Mg + Ca) in the starting solution.